Research Article

Received: 23 November 2011 Revised: 3 February 2012 Accepted: 6 February 2012 Published online in Wiley Online Library:

(wileyonlinelibrary.com) DOI 10.1002/jctb.3778

Kinetic study of the partial hydrogenation of 1-heptyne on tungsten oxide supported on alumina

María Maccarrone,[a] Gerardo Torres,[b] Cecilia Lederhos,[a] Juan Badano,[a] Carlos Vera,[a,b] Mónica Quiroga[a,b] and Juan Yori[a,b]*

Abstract

BACKGROUND: Partial hydrogenation of alkynes have industrial and academic relevance on a large scale; industries such as petrochemical, pharmacology and agrochemical use these compounds as raw material. Typical commercial catalysts contains palladium. Finding an economic, active and selective catalyst for the production of alkenes via partial hydrogenation of alkynes is thus an important challenge. On the other hand, the literature on kinetic studies of partial hydrogenation of heavy alkynes is scarce. So the main objectives of this work were to prepare a cheaper catalyst based on low W loading, and study the kinetic of the partial hydrogenation of 1-heptyne. A pseudo-homogeneous and six heterogeneous kinetic models were analyzed. The catalyst was characterized by ICP, XPS, DRX, TPR and hydrogen chemisorption techniques.

RESULTS: The characterization results indicate that only WO_x species are present on the alumina surface. The WO_x/Al_2O_3 catalyst was active and selective for producing 1-heptene even at low reaction temperatures, the partial hydrogenation of 1-heptyne proceeds via two irreversible reactions in parallel.

CONCLUSION: The best fit of the experimental data was achieved with a heterogeneous Langmuir-Hinshelwood-Hougen-Watson model in which the rate controlling step is the dissociative adsorption of hydrogen. The activation energy was estimated as E_{H2} =34.8 kJ mol^{-1}.

Keywords: selective hydrogenation; alkyne; tungsten catalysts; kinetic study

INTRODUCTION

A subset of the group of reactions collectively known as 'selective hydrogenation reactions' is that of 'partial hydrogenation reactions'. In these reactions highly unsaturated organic compounds are partially hydrogenated in order to prevent undesired reactions or to produce other compounds which are raw materials for organic synthesis and petrochemistry. In the case of the manufacture of high added value final products or intermediates for fine chemistry, the reactions involved have become of both industrial and academic importance.[1] Typical products of partial hydrogenation are the alkenes that arise from to the partial saturation of alkynes and aromatic compounds. There exists a high number of important products that are used in the food (flavours), pharmaceutical (sedatives, anesthetics, vitamins), cosmetics (fragrances), plastics (resins and polymers) and lubricants industries. Many of these speciality compounds are complex molecules that can have biological activity.[2]

Certain transition metals anchored on different supports have been demonstrated to be very active and selective catalysts for this type of reaction. They also have the advantage of requiring relatively mild reaction conditions. It is well documented that palladium is a highly active hydrogenation catalyst.[3] The Lindlar catalyst ($Pd/CaCO_3$, 5%(w/w) Pd modified with $Pb(OAc)_2$) is a classical commercial catalyst that has been in use since 1952 for this type of reaction.[4] $Pd\text{-}Co/Al_2O_3$ and $Pd\text{-}W/Al_2O_3$ bimetallic catalysts showed activity in the liquid phase selective hydrogenation of cyclopentadiene to cyclopentene.[5] On the other hand, at mild conditions during the partial hydrogenation of 1-heptyne, a Rh(I) anchored complex exhibited higher activity than the Lindlar catalyst and than a Pd(II) complex.[6]

Different supports for the palladium metal phase have been used (alumina, coal, silica)[7–9] and modifications to the metal phase chemical nature[10] or particle size[11–13] have been introduced. One of the key problems associated with palladium is its high cost, which imposes appreciable requirements on catalyst reuse, catalyst regeneration and palladium recovery from spent materials. It is therefore of great interest to search for alternative partial hydrogenation active metals that can prove to be of similar activity and selectivity but of reduced cost. In this way the use of cheaper metals such as nickel, is of great industrial interest.[14–19]

* *Correspondence to: Juan Yori, INCAPE, Santiago del Estero 2654, (S3000AOJ) Santa Fe, Argentina. E-mail: jyori@fiq.unl.edu.ar*

a *INCAPE -CONICET, Instituto de Investigaciones en Catálisis y Petroquímica Santiago del Estero 2654, S3000AOJ Santa Fe, Argentina*

b *Facultad de Ingeniería Química, Universidad Nacional del Litoral, Santiago del Estero 2829, S3000AOJ Santa Fe, Argentina*

A nickel complex anchored on alumina was shown to be more active and sulfur resistant for the hydrogenation of cyclohexene than the homogeneous one.[20]

In recent work it was found that very high activities and selectivities for the partial hydrogenation of a long chain terminal alkyne can be accessed using W and W-Pd catalysts,[21] noting that important variations in activity and selectivity can be obtained when varying catalyst pretreatment conditions. Finding an economic, active and selective catalyst for the production of alkenes via partial hydrogenation of alkynes is thus an important challenge. The literature on kinetic analysis of partial hydrogenation of heavy alkynes is limited.[22–24] The main objective of this work was to study the kinetic of the 1-heptyne partial hydrogenation reaction in the liquid phase using tungsten supported on γ-alumina. A stirred batch reactor was used for the kinetic tests. Several heterogeneous kinetic models were tested in order to determine the global mechanism and its kinetic parameters.

EXPERIMENTAL

Catalyst preparation

The catalyst was prepared by an incipient wetness technique using Ketjen CK300 γ-Al_2O_3 as support (cylinders of 1.5 mm calcined at 823 K for 4 h, 180 $m^2\ g^{-1}$ BET surface area). An aqueous acid solution of phosphotungstic acid $H_3PO_4.12WO_3$ (Fluka, Cat. N° 79 690) at pH = 1 was used to prepare the catalyst. The volume and concentration of the impregnating solution were adjusted to achieve 2.4%(w/w) W on the final catalyst. After impregnation, the solid was dried for 24 h at 373 K and then calcined in flowing air at 823 K for 3 h. Before reaction the catalysts was reduced in flowing hydrogen (105 mL min^{-1}) at 673 K for 1 h. The prepared catalyst was named WO_x/Al_2O_3.

Catalyst characterization

The tungsten and phosphorous contents were determined by inductively coupled plasma (ICP) analysis in an OPTIMA 21 200 Perkin Elmer equipment. The superficial electronic state of the metal was studied by X-ray photoelectron spectroscopy (XPS) assessment of the W $4f_{7/2}$ peak. XPS measurements were made in a Multitech UniSpecs XR-50 unit with a dual Mg/Al X-ray source and an hemisphere analyzer SPECS PHOIBOS 150. The sample was treated at 673 K *ex situ* with a hydrogen flow for 1 h and *in situ* in the load camera of the instrument with a H_2/Ar (5% (v/v)) flow for 10 min. X-ray diffraction (XRD) measurements of the sample were obtained using a Shimadzu XD-1 instrument with Ni filtered CuKα radiation ($\lambda = 1.5405$ Å) in the $15 < 2\theta < 85^\circ$ range and with a scan speed of $1^\circ\ min^{-1}$. The sample was ground to a fine powder and reduced in hydrogen flow. After cooling in hydrogen it was immediately put into the equipment chamber for analysis. The TPR test was performed in a Ohkura 2002 S apparatus equipped with a thermal conductivity detector. Before TPR measurement, the sample was treated *in situ* at 673 K for 30 min under an oxygen flow (AGA purity 99.99%). After that, it was cooled to 298 K in an argon flow, the temperature increased to 1223 K at 10 K min^{-1} in a H_2/Ar gas flow (5% (v/v)). Hydrogen chemisorption was performed by means of the dynamic pulse method using a Micromeritics Auto Chem II apparatus equipped with a thermal conductivity detector. 0.2 g of the sample were reduced for 1 h *in situ* at 673 K using a H_2/Ar (5% v/v) flow. Finally, hydrogen chemisorption was performed until total saturation of the sample.

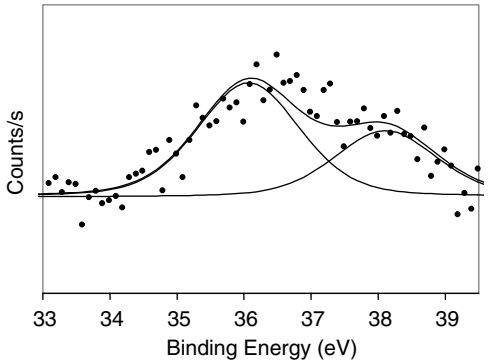

Figure 1. XPS W $4f_{7/2}$ spectra of the WO_x/Al_2O_3 catalyst reducet at 673 K.

Catalytic tests

The partial hydrogenation of 1-heptyne was carried out in a stainless steel stirred batch reactor equipped with a magnetically coupled stirrer with two blades in counter-rotation that was operated at 800 rpm. The tests were performed using the following conditions: 1.4 bar hydrogen pressure, 293–323 K reaction temperature, 60–120 mesh particle size. The reactant, 1-heptyne (Fluka, Cat. No. 51 950, >98%), was dissolved to 2% (v/v) in toluene (Merck, Cat. No. TX0735-44, >99%) to form a stock solution. 75 mL of this stock solution and catalyst sample WO_x/Al_2O_3 of 0.3 g were then used in the different catalytic tests. The evolution of the concentration of reactants and products as a function of time was obtained by means of sampling and gas cromatography analysis with a flame ionization detector (FID) and a 30 m, J&W INNOWax 19 091N-213 capillary column.

RESULTS AND DISCUSSION

Catalyst characterizaction

The W metal loading of the prepared catalysts was 1.61 (%w/w) as determined by ICP. After the calcination and reduction procedure, no phosphorous was detected in the catalyst by ICP analysis, indicating that it was totally eliminated by the thermal steps. No hydrogen consumption was detected for the WO_x/Al_2O_3 catalyst during the chemisorption analysis, in total accordance with previously reported results,[25,26] indicating that at the conditions of the test there are no surface sites capable of adsorbing hydrogen.

Figure 1 shows the XPS spectra (BE of W $4f_{7/2}$) of the WO_x/Al_2O_3 catalyst. According to literature references, the binding energy (BE) of W $4f_{7/2}$ in the case of metallic tungsten W^0 is 34.0 eV.[27] The catalyst reduced at 673 K has a W $4f_{7/2}$ signal at 36.1 eV. According to previous work this value of BE indicates that tungsten is present on the alumina surface as an electron-deficient species, W^{6+}.[28,29] The XRD diffractogram of the catalyst (not shown) only had peaks due to γ-alumina at $2\theta = 37.7$, 46.0 and 67.0°.[30,31] The absence of signals in the $20^\circ < 2\theta < 30^\circ$ region suggests that there is no tungsten oxide present as a crystalline segregated phase, as could be expected from the low W surface concentration on the catalyst.[32]

Figure 2 shows the TPR profile for the catalyst. The main reduction peak starts at 900 K and there is a shoulder at 1143 K. The maximum hydrogen consumption occurs at temperatures higher than 1200 K. Several authors[32–34] reported that highly dispersed WO_x bound to alumina through strong bonds had reduction peaks at high temperatures (950–1300 K). We can assign the observed reduction peak to the reduction of amorphous WO_x species,

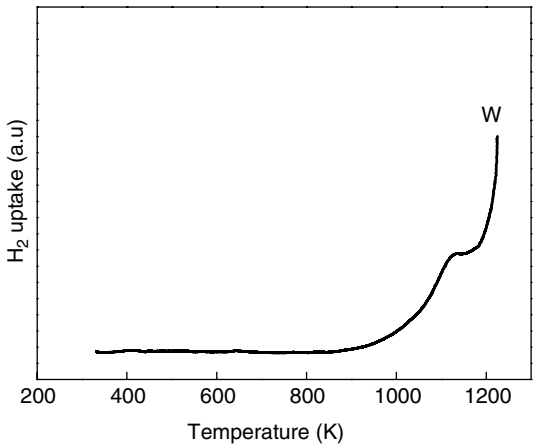

Figure 2. TPR trace of the WO_x/Al_2O_3 catalyst.

confirming the results found by XPS. We can therefore conclude that after pretreatment the catalyst is formed by WO_x species in intimate contact with the alumina support. The characterization thus suggests the presence of only one type of active site.

Catalytic results

1-heptyne partial hydrogenation

Before considering kinetic expressions or comparing catalyst performances, it is necessary to check whether the selected reaction system operates under kinetic regime. The possibility of external and internal diffusional limitations during the catalytic tests was thus experimentally assessed. In order to eliminate external difussional limitations, experiences were carried out using different stirring speeds, in the range 180–1400 rpm. It was found that at stirring rates higher than 500 rpm 1-heptyne conversion values remained constant, i.e. external diffusional limitations were absent. Therefore a stirring rate of 800 rpm was chosen for all the kinetic tests. On the other hand in order to ensure that the catalytic results were not influenced by both external and intra-particle mass transfer limitations, the catalyst pellets were milled to samples of different particle sizes: a fraction bigger than 100 mesh ($<$ 150 μm), a fraction of 60–100 mesh (250–150 μm) and pellets of 1500 μm (not milled). The values of 1-heptyne conversion obtained were the same for the two milled fractions indicating the absence of external and internal diffusional limitations. Then particles with sizes smaller than 250 μ were used in all tests.

In order to determine the orders of reaction for each reactant (1-heptyne and hydrogen) and the apparent activation energy of the system, tests were performed in which the partial pressure of hydrogen, the initial concentration of 1-heptyne and the temperature of reaction were varied. In order to test the influence of the cited variables on the initial reaction rate a pseudohomogeneous model of reaction was proposed. The kinetic reaction rate was assumed to obey a power law of the form:

$$r_A^0 = k.(C_A^0)^{\alpha}.(P_{H2})^{\beta} \quad (1)$$

where $r_A{}^0$ is 1-heptyne initial hydrogenation rate, k is specific reaction rate constant, $C_A{}^0$ is initial concentration of 1-heptyne, P_{H2} is partial pressure of hydrogen, α is order of reaction with respect to 1-heptyne and β is order of reaction with respect to hydrogen. In the case of the reaction rate specific constant, an

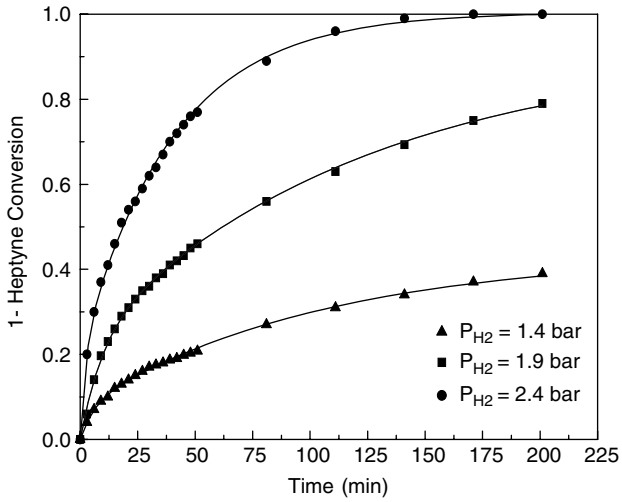

Figure 3. Effect of the hydrogen partial pressure on the reaction rate.

Arrhenius expression was used:

$$k = A.e^{\frac{-E_A}{R.T}} \quad (2)$$

where A is Arrhenius preexponential factor, R is ideal gas universal constant (0.082 L atm mol^{-1} K^{-1}), E_A is apparent activation energy and T is absolute temperature.

Influence of hydrogen partial pressure

The catalytic tests were performed at hydrogen partial pressures of 1.4, 1.9 and 2.4 bar, keeping all other variables constant (initial concentration of 1-heptyne, catalyst mass, temperature of reaction and solvent volume). The partial pressure of hydrogen was calculated as the difference between the total pressure and the partial pressure of the solvent (toluene). For this calculation the vapor pressure of 1-heptyne and other products were considered negligible. The vapor pressure of toluene at 303 K was 0.048 bar according to Antoine's equation. The experimental values of conversion of 1-heptyne as a function of the reaction time at different values of the partial pressure of hydrogen are plotted in Fig, 3. From the plot of ln (r^0_A) vs. ln (P_{H2}) the reaction order of hydrogen was calcualted as 2.4.

Influence of the initial concentration of 1-heptyne

Catalytic tests were performed with initial values of concentration of 1-heptyne of 0.1019, 0.1528 and 0.2038 mol L^{-1} and keeping the rest of the reaction variables constant (partial pressure of hydrogen, catalyst mass, reaction temperature and solvent volume). The values of conversion of 1-heptyne obtained as a function of the reaction time at different values of the initial concentration of 1-heptyne are plotted in Fig. 4. From the plot of ln (r^0_A) vs. ln (C^0_A) the order of reaction of 1-heptyne was calculated as -1.

Influence of the reaction temperature

The catalytic tests were performed at reaction temperatures of 293, 303 and 323 K, while keeping the rest of the variables constant (initial concentration of 1-heptyne, partial pressure of hydrogen, catalyst mass and solvent volume). The experimental values of

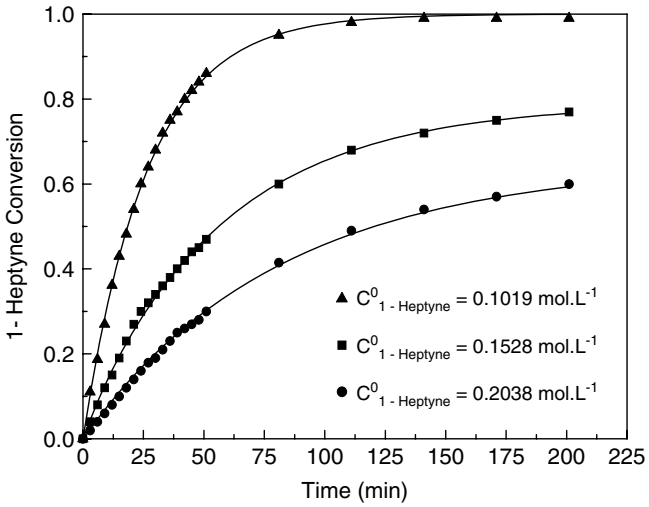

Figure 4. Effect of the initial concentration of 1-heptyne on the reaction rate.

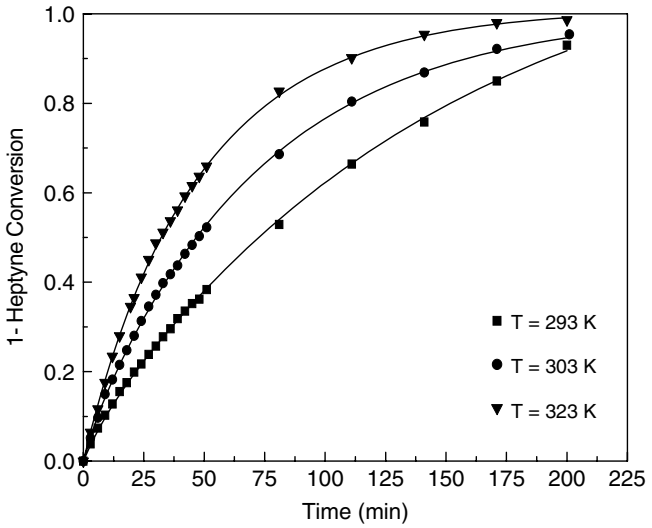

Figure 5. Effect of the reaction temperature on the reaction rate.

conversion of 1-heptyne as a function of reaction time at different reaction temperature are plotted in Fig. 5. It can be seen that the reaction rate is increased with the reaction temperature. When equation (1) is linearized the apparent activation energy of the reaction system (E_A) can be estimated by linear regression. The value of the apparent energy of activation obtained from the plot of ln (r^0_A) as a function of $1/T$ was 30.4 kJ mol^{-1}.

Kinetic modeling

It was postulated that the formation of n-heptane occurred not only in a consecutive but also in a parallel way.[23] Fig. 6(a) shows the proposed kinetic scheme for the 1-heptyne reaction. The proposed scheme is a series–parallel network composed of three hydrogenation reactions that are originally considered reversible. The equilibrium constants for each of the previous reactions were calculated using the method of group contribution of Joback.[35] The calculated values at 323 K were $k_1 = 3.35 \times 10^{21}, k_2 = 1.87 \times 10^{35}$ and $k_3 = 5.58 \times 10^{13}$. These values indicate that the elementary reactions in Fig. 6(a) can be considered as irreversible. The experimentally obtained values of total conversion of 1-heptyne confirmed this prediction. Experimentally, it is observed that while 1-heptyne is present in the reaction medium, 1-heptene concentration always increases, showing a higher concentration than n-heptane. After all 1-heptyne was consumed, 1-heptene concentration begins to decrease very slowly and n-heptane concentration increases equally. These profiles are consistent with two reaction schemes: (i) two parallel irreversible reactions (steps 1 and 3), and (ii) series-parallel irreversible reactions, with a k_1/k_2 value higher than 100. The latter considerations, allow us to disregard step 2. Therefore a simplified network of parallel reactions for 1-heptyne hydrogenation can be assumed in Fig. 6(b).

Langmuir-Hinshelwood-Hougen-Watson (LHHW) Models

Models of heterogeneous reactions were outlined using the Langmuir-Hinshelwood-Hougen-Watson formalism (LHHW models). Taking into account the previously presented characterization results of WO_x/Al_2O_3, in all the models only one active site was considered to be present. Six different models with their respective basic hypotheses are presented in Table 1. The elementary steps with H_2 dissociative or non-dissociative adsorption reaction mechanism are presented in Table 1(b). The following mass balances for components in the liquid phase were considered for the reaction

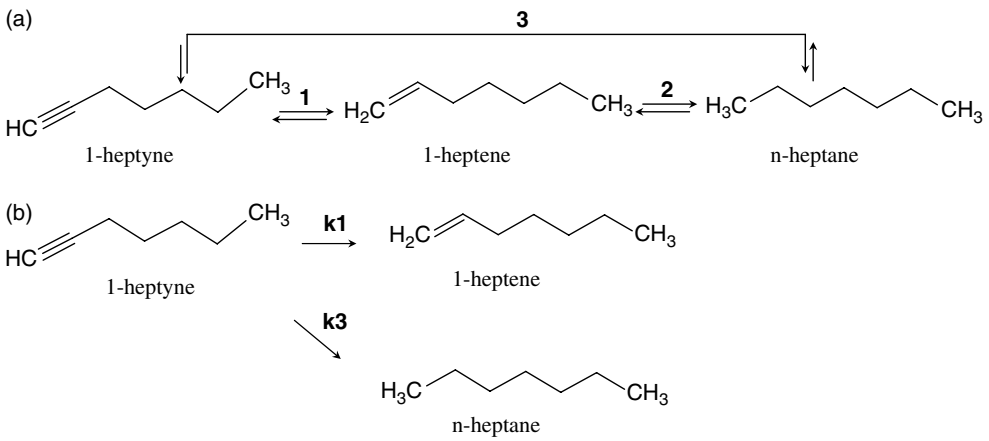

Figure 6. Scheme of the 1-heptyne hydrogenation reactions: (a) reversible; (b) irreversible.

Table 1. (a) LHHW kinetic models

Model	Hypothesis of the model	Simplified rate	Parameters
I	Controlling step: adsorption of H_2. Dissociative adsorption of H_2.[33] Competitive adsorption of 1-heptyne and H_2. Total coverage of active sites.	$r = \frac{P_3}{[C_A + P_1.C_B + P_2.C_C]^2}$	$P_1 = \frac{K_B}{K_A}P_2 = \frac{K_C}{K_A}P_3 = \frac{k_{H_2}.C_{H_2}.C_S^2}{K_A^2}$
II	Controlling step: adsorption of 1-Heptyne. Dissociative adsorption of H_2.[33] Competitive adsorption of 1-heptyne and H_2. Total coverage of active sites.	$r = \frac{P_6.C_A}{[1 + P_4.C_B + P_5.C_C]}$	$P_4 = \frac{K_B}{\sqrt{K_{H_2}.C_{H_2}}}P_5 = \frac{K_C}{\sqrt{K_{H_2}.C_{H_2}}}P_6 = \frac{k_A.C_S}{\sqrt{K_{H_2}.C_{H_2}}}$
III	Controlling step: surface chemical reaction. Dissociative adsorption of H_2.[33] Competitive adsorption of 1-heptyne and H_2. Total coverage of active sites.	$r_1 = \frac{P_{10}.C_A}{[1 + P_7.C_A + P_4.C_B + P_5.C_C]^3}$	$P_7 = \frac{(1 + K.K_{H_2}.C_{H_2}).K_A}{\sqrt{K_{H_2}.C_{H_2}}}P_{10} = \frac{k_1.K_A.C_S^3}{\sqrt{K_{H_2}.C_{H_2}}}P_{11} = \frac{k_3.K_A.K.C_S^3}{\sqrt{K_{H_2}.C_{H_2}}}$
		$r_3 = \frac{P_{11}.C_A}{[1 + P_7.C_A + P_4.C_B + P_5.C_C]^3}$	
IV	Controlling step: adsorption of H_2. Non dissociative adsorption of H_2.[34] Competitive adsorption of 1-heptyne and H_2. The active sites are not completely covered.	$r = \frac{P_{12}}{[1 + K_A.C_A + K_B.C_B + K_C.C_C]}$	$P_{12} = k'_{H_2}.C_{H_2}.C_S$
V	Controlling step: adsorption of 1-Heptyne. Non dissociative adsorption of H_2.[34]Competitive adsorption of 1-heptyne and H_2. The active sites are not completely covered.	$r = \frac{P_{14}.C_A}{[1 + P_{13} + K_B.C_B + K_C.C_C]}$	$P_{13} = K^*_{H_2}.C_{H_2}P_{14} = k_A.C_S$
VI	Controlling step: surface chemical reaction. Non dissociative adsorption of H_2.[34] Competitive adsorption of 1-heptyne and H_2. The active sites are not completely covered.	$r_1 = \frac{P_{16}.C_A}{[1 + P_{13} + P_{15}.C_A + K_B.C_B + K_C.C_C]^2}$	$P_{15} = (1 + K^*.K^*_{H_2}.C_{H_2}).K_A$
		$r_3 = \frac{P_{17}.C_A}{[1 + P_{13} + P_{15}.C_A + K_B.C_B + K_C.C_C]^2}$	$P_{16} = k_1.K_A.K^*_{H_2}.C_{H_2}.C_S^2$ $P_{17} = k_3.K_A.K^*.K^{*2}_{H_2}.C^2_{H_2}.C_S^2$

A: 1-heptyne; B: 1-heptene; C: n-heptane.

Table 1. (b) Elementary steps with H_2 dissociative or non-dissociative adsorption reaction mechanism

H_2 dissociative adsorption.		H_2 non dissociative adsorption.	
$H_2 + 2S \Leftrightarrow 2\,HS \quad K_{H_2} = \frac{C^2_{HS}}{C_{H_2}.C_S^2}$	(3).	$H_2 + S \Leftrightarrow H_2S \quad K^*_{H_2} = \frac{C_{H_S}S}{C_{H_2}.C_S}$	(10).
$A + S \Leftrightarrow AS \quad K_A = \frac{C_{AS}}{C_A.C_S}$	(4).	$A + S \Leftrightarrow AS \quad K_A = \frac{C_{AS}}{C_A.C_S}$	(11).
$AS + 2HS \rightarrow BS + 2S \;\; K_1 = \infty$	(5).	$AS + H_2S \rightarrow BS + S \quad K_1 = \infty$	(12).
$AS + 2HS \Leftrightarrow AH_2S + 2S \quad K = \frac{C_{AH_2S}.C_S^2}{C_{AS}.C^2_{HS}}$	(6).	$AS + H_2S \Leftrightarrow AH_2S + S \quad K^* = \frac{C_{AH_2S}.C_S}{C_{AS}.C_{H_2S}}$	(13).
$AH_2S + 2\,HS \rightarrow CS + 2S \quad K_3 = \infty$	(7).	$AH_2S + H_2S \rightarrow CS + S \quad K_3 = \infty$	(14).
$BS \Leftrightarrow B + S \frac{1}{K_B} = \frac{C_B.C_S}{C_{BS}}$	(8).	$BS \Leftrightarrow B + S \quad \frac{1}{K_B} = \frac{C_B.C_S}{C_{BS}}$	(15).
$CS \Leftrightarrow C + S \quad \frac{1}{K_C} = \frac{C_C.C_S}{C_{CS}}$	(9).	$CS \Leftrightarrow C + S \quad \frac{1}{K_C} = \frac{C_C.C_S}{C_{CS}}$	(16).

scheme of Fig. 6(b):

$$dC_A/dt = -r_1 - r_3 \quad (17)$$

$$dC_B/dt = r_1 \quad (18)$$

$$dC_C/dt = r_3 \quad (19)$$

where A=1-heptyne, B=1-heptene and C=n-heptane. The initial conditions were: t = 0 min, $C^0{}_A = 0.1528$ mol L^{-1}, $C^0_B = C^0_C =$ 0 mol L^{-1}.

Numerical resolution and statistics

The system of differential equations (17)–(19) was solved numerically using the Runge–Kutta–Merson algorithm. The model parameter estimation was performed by a non-linear regression, using a Levenberg–Marquardt algorithm which minimized the objective function.

$$SCD = \sum_j^n \left(C_{i,j} - C_{i,j}^{CALC}\right)^2 \quad (20)$$

where $C_{i,j}$ and $C_{i,j}^{CALC}$ are the experimental and the predicted concentration values, respectively, *i* is the chemical compound and *j* is the reaction time. The model adequacy and the discrimination between models were determined using the model selection criterion (MSC), according to the following equation.

$$MSC = \ln\left(\frac{\sum_j^n \left(C_{i,j} - \overline{C}_i\right)^2}{\sum_j^n \left(C_{i,j} - C_{i,j}^{CALC}\right)^2}\right) - \left(\frac{2p}{n}\right) \quad (21)$$

where $\overline{C}_i$ is the average relative concentration; p is the amount of parameters fitted and n is the number of experimental data. In order to compare different models, the selected one is that leading to the highest *MSC* value. The standard deviation (S) was calculated with the following equation:

$$S = \sqrt{s^2} = \sqrt{\frac{\sum_j^n (C_{i,j} - C_{i,j}^{CALC})^2}{n-p}} \quad (22)$$

Kinetic modeling results

Models II, III, V and VI of Table 1 were discarded because they cannot explain the negative order in 1-heptyne and the positive order in hydrogen experimentally obtained. The value estimated for the parameters in models I and IV are indicated in Table 2. An analysis was made for discriminating between the different models from a statistical point of view. The results of the discrimination analysis are summarized in Table 2. It can be concluded that the best fit is achieved with model I-B. In this model the value of P_2 is equal to zero, indicating that n-heptane is not adsorbed.

Figure 7 contains experimental values of the concentration of 1-heptyne, 1-heptene and n-heptane along with theoretical values (solid line) estimated with model I-B, as a function of time. A good fit between the two sets of values can be seen. The same regression with model I-B was done with experimental data obtained at other reaction temperatures in the 293–323 K range. In all cases and as a consequence of the fit, parameters different from zero were obtained for a confidence interval of 95% and with values of the MSC parameter greater than 4.0. The thermodynamical consistency of the P_1 and P_3 parameters was graphically evaluated by plotting ln P_1 and ln P_3 as a function of 1/T. In both cases a straight line was obtained (Figs 8 and 9) indicating that the constants have an Arrhenius dependence on temperature. The slopes of the straight lines correspond to the values of the enthalpies of adsorption of 1-heptyne and 1-heptene and the value of the energy of activation for the dissociative adsorption of hydrogen on the active sites. Considering the definition of P_1 and P_3, the following equations can be obtained.

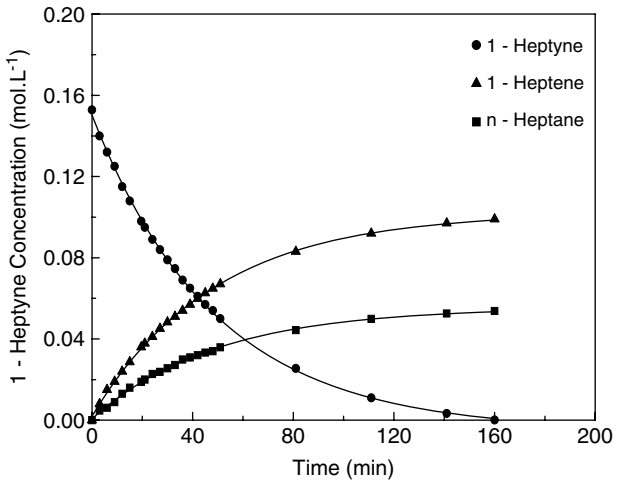

Figure 7. Experimental points and theoretical curves obtained with the heterogeneous kinetic model. Reaction conditions: 1.4 bar of H_2, 323 K, catalyst mass 0.3 g, 800 rpm.

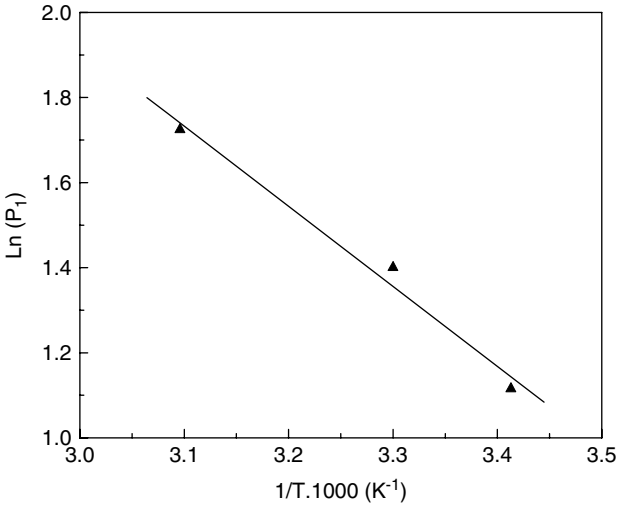

Figure 8. Dependence of the P_1 parameter on temperature.

$$P_1 = \frac{K_B}{K_A} = \left(\frac{A_B}{A_A}\right).\mathrm{Exp}\left[\frac{|\Delta H_B| - |\Delta H_A|}{R.T}\right] \quad (23)$$

$$P_3 = \frac{C_{H2}.k_{H2}.C_S^2}{K_A^2} = \left(\frac{C_{H2}.A_{H2}.C_S^2}{A_A^2}\right).$$
$$\mathrm{Exp}\left[\frac{-(E_{H2} + 2.|\Delta H_A|)}{R.T}\right] \quad (24)$$

Table 2. Estimated parameters and model discrimination for WO_x/Al_2O_3

Model	Option	Estimated parameters(*)	SCD	MSC	Parameter	Parameter sign	Discrimination	Viability
I	A	$P_1 = 47.9030574 \pm 228.7645946$	0.00044	5.20	P_1	(+)	IC < 0, CL > VE	Non viable
		$P_2 = -84.6397138 \pm 448.4094668$			P_2	(−)		
		$P_3 = 0.000107361701 \pm 0.000034179$			P_3	(+)	IC < 0, CL > VE	
							IC > 0, CL < VE	
	B	$P_1 = 5.60827241 \pm 0.41113674$	0.00044	5.23	$P_2 = 0$			Viable
		$P_2 = 0$			P_1	(+)	IC > 0, CL < VE	
		$P_3 = 0.000108055877 \pm 0.000011179$			P_3	(+)	IC > 0, CL < VE	
IV	A	$K_A = 529.880207 \pm 15894.8078$	0.00095	4.4	K_A	(+)	IC < 0, CL > VE	Non viable
		$K_B = -52677.0918 \pm 2009446.9869$			K_B	(−)	IC < 0, CL > VE	
		$K_C = 176460.7316 \pm 2013126.837$			K_C	(+)	IC < 0, CL > VE	
		$P_{12} = 1.42293014 \pm 43.27998806$			P_{12}	(+)	IC < 0, CL > VE	
	B	$K_A = 350.720207 \pm 14560.0078$	0.00091	4.5	K_A	(+)	IC < 0, CL > VE	Non viable
		$K_B = 0$			$K_B = 0$			
		$K_C = 123520.5320 \pm 1533126.600$			K_C	(+)	IC < 0, CL > VE	
		$P_{12} = 1.01111236 \pm 40.28897706$			P_{12}	(+)	IC < 0, CL > VE	

Reaction conditions: $P_{H2} = 1.4$ bar, T=323 K, $w_{cat} = 0.3$ g, solvent = toluene, stirring rate = 800 rpm, $C^0_{1-heptyne} = 0.1528$ mol.L^{-1}.
(*) 95% confidence interval. IC: confidence interval. CL: confidence level. VE: estimated value of the parameter.

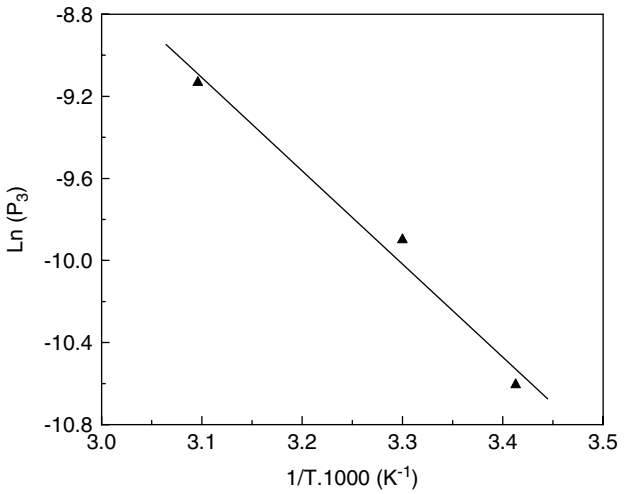

Figure 9. Dependence of the P_3 parameter on temperature.

In Equations (23) and (24) the enthalpies of adsorption of 1-heptyne and 1-heptene were expressed in absolute values.The obtained values from the slopes of the lines in Figs 8 and 9 were:

$$|\Delta H_B| - |\Delta H_A| = -15.6 \text{KJ mol}^{-1} \quad (25)$$

$$E_{H2} + 2.|\Delta H_A| = 66 \text{KJ mol}^{-1} \quad (26)$$

From the results it could be concluded that:

(1) Model I-B assumes dissociative adsorption of hydrogen as the rate-controlling step of reaction and a single type of active sites with total coverage, is the one that best fits experimental data with statistical and thermodynamic consistency.
(2) The model does not allow the enthalpies of adsorption of 1-heptyne and 1-heptene and the activation energy for the adsorption of hydrogen to be obtained directly.
(3) From Equation (25) it can be inferred that the enthalpy of adsorption of 1-heptyne is greater than that of 1-heptene, in agreement with the information available in the literature on the partial hydrogenation of alkynes.[36]
(4) If we suppose that the enthalpy of adsorption of 1-heptene is negligible, in accord with the experimental results, a value of the enthalpy of adsorption for 1-heptyne can be obtained from Equation (25) (−15.6 kJ mol^{-1}). Introducing this value in Equation (26) a value of E_{H2} of 34.8 kJ mol^{-1} can be estimated. This value is high considering that it was obtained by assuming that the enthalpy of alkene adsorption is negligible. It can then be concluded that the active sites of the catalyst are preferentially occupied by 1-heptyne. This explains why an increase in the partial pressure of hydrogen has a beneficial effect on the reaction rate. In the case of 1-heptyne, an increase in the initial concentration of 1-alkyne has a negative effect because it decreases the surface concentration of adsorbed hydrogen. Finally it can be stated that these results coincide with those found in the tests of chemisorption of hydrogen on the W/Al_2O_3 catalyst, when no adsorption could be detected at room temperature. On the other hand, from Equation (25) it is possible to calculate the activation energy for the dissociative hydrogen adsorption ($E_{H2} = 34.8$ kJ mol^{-1}) that is in good agreement with the 'apparent' value determined from experimental data assuming a pseudohomogeneus model (30.4 kJ mol^{-1}).
(5) The relatively high selectivity values to alkene (70%) of the catalyst may be because: (i) apparently the only adsorbed species are 1-heptyne and hydrogen (while 1-heptyne is present in the reaction medium); and (ii) the reaction rate of partial hydrogenation is higher than the total hydrogenation ones.

CONCLUSIONS

A WO_x/Al_2O_3 catalyst with low W content (1.61 (%w/w)) was prepared and it proved to be a viable and economic alternative for the partial hydrogenation of 1-heptyne. The 1-heptyne hydrogenation reaction over WO_x/Al_2O_3 catalyst proceeded via a network of two paralell irreversible hydrogenation reactions. A

heterogeneous LHHW model in which the rate controlling step is the dissociative adsorption of hydrogen was found to give the best fit of the experimental data. The reaction kinetic is expressed by:

$$r = \frac{P_3}{[C_A + P_1.C_B]^2}$$

Assuming that adsorption enthalpy of 1-heptene is negligible, a value of -15.6 kJ mol^{-1} can be estimated for the enthalpy of adsorption for 1-heptyne and the 34.8 kJ mol^{-1} for the activation energy for the hydrogen adsorption.

ACKNOWLEDGEMENTS

The experimental asistance of C. A. Mázzaro and the financial support provided by UNL and CONICET of Argentina are gratefully acknowledged.

REFERENCES

1 L'Argentière PC, Cagnola EA, Quiroga ME and Liprandi DA, A palladium tetra-coordinated complex as catalyst in the selective hydrogenation of 1-heptyne. *Appl Catal A: Gen* **226**:253–263 (2002).
2 Lennon D, Marshall R, Webb G and Jackson SD, The effects of hydrogen concentration on propyne hydrogenation over a carbon supported palladium catalyst studied under continuous flow conditions. *Studies Surf Sci Catal* **130**:245–250 (2000).
3 Nishimura S, *Handbook of Heterogeneous Catalytic Hydrogenation for Organic Synthesis*. John Wiley & Sons, Inc., New York (2001).
4 Lindlar H and Dubuis R, Palladium catalyst for partial reduction of acetylenes. *Org Synth* **46**:89–92 (1966).
5 Fígoli NS, Barberis JP and L'Argentière PL, Selective hydrogenation of cyclopentadiene over supported metal catalysts. *J Chem Technol Biotechnol* **67**:72–76 (1996).
6 Quiroga ME, Liprandi DA, L' Argentière PL and Cagnola EA, Obtaining 1-heptene from 1-heptyne semihydrogenation with an anchored rhodium complex on different supports as catalyst. *J Chem Technol Biotechnol* **80**:158–163 (2005).
7 Lederhos CR, L'Argentière PC and Fígoli NS, 1-Heptyne selective hydrogenation over Pd supported catalysts. *Ind Eng Chem Res Dev* **44**:1752–1756 (2005).
8 Bennett JA, Creamer NJ, Deplanche K, Macaskie LE, Shannon IJ and Wood J, Palladium supported on bacterial biomas as a novel heterogeneous catalyst: a comparison of Pd/Al_2O_3 and bio-Pd in the hydrogenation of 2-pentyne. *J Chem Eng Sci* **65**:282–290 (2010).
9 Sárkány A, Beck A, Horváth A, Révay Zs and Guczi L, Acetylene hydrogenation on sol-derived Pd/SiO_2. *Appl Catal A: Gen* **253**:283–292 (2003).
10 Anderson JA, Mellor JL and Wells RPK, Pd catalysed hexyne hydrogenation modified by Bi and by Pb. *J Catal* **261**:208–216 (2009).
11 Evangelisti C, Panziera N, D'Alessio A, Bertinetti L, Botavina M and Vitulli G, New monodispersed palladium nanoparticles stabilized poly-(N-vinyl-2-pyrrolidone): preparation, structural study and catalytic properties. *J Catal* **272**:246–252 (2010).
12 Mastalir A and Király Z, Pd nanoparticles in hydrotalcite: mild and highly selective catalysts for alkyne semihydrogenation. *J Catal* **220**:372–381 (2003).
13 Jung A, Jess A, Schubert T and Schütz W, Performance of carbon nanomaterial (nanotubes and nanofibres) supported platinum and palladium catalysts for the hydrogenation of cinnamaldehyde and of 1-octyne. *Appl Catal A: Gen* **362**:95–105 (2009).
14 Lederhos CR, Badano JM, Quiroga ME, Coloma-Pascual F and L'Argentière PC, Influence of Ni addition to a low-loaded palladium catalyst on the selective hydrogenation of 1-heptyne. *Quim Nova*. **33**:816–820 (2010).
15 Abelló S, Verboekend D, Bridier B and Pérez-Ramírez J, Activated takovite catalysts for partial hydrogenation of ethyne, propyne, and propadiene. *J Catal* **259**:85–95 (2008).
16 Alonso F, Osante I and Yus M, Highly Stereoselective semihydrogenation of alkynes promoted by nickel(0) nanoparticles. *Adv Synth Catal* **348**:305–308 (2006).
17 Dhakshinamoorthy A and Pitchumani K, Clay entrapped nickel nanoparticles as efficient and recyclable catalysts for hydrogenation of olefins. *Tetrahed Lett* **49**:1818–1823 (2008).
18 Zhao ZF, Wu ZJ, Zhoy LX, Zhang MH, Li W and Tao KY, Synthesis of a nano-nickel catalyst modified by ruthenium for hydrogenation and hydrodechlorination. *Catal Commun* **9**:2191–2124 (2008).
19 Choi J and Yoon NM, An excellent nickel boride catalyst for the cis-selective semihydrogenation of acetylenes. *Tetrahed Lett* **37**:1057–1060 (1996).
20 L'Argentière PL, Cagnola EA, Cañón MG, Liprandi DA and Marconetti DV, A nickel tetra-coordinated complex as catalyst in heterogeneous hydrogenation. *J Chem Technol Biotechnol* **71**:285–290 (1998).
21 Lederhos CR, Maccarrone MJ, Badano JM, Coloma-Pascual F, Yori JC and Quiroga ME, Hept-1-yne partial hydrogenation reaction over supported Pd and Wcatalysts. *Appl Catal A: Gen* **396**: 170–176 (2011).
22 Alves JA, Bressa SP, Martínez OM and Barreto GF, Kinetic study of the liquid-phase hydrogenation of 1-butyne over a commercial palladium/alumina catalyst. *J Chem Eng* **125**:131–138 (2007).
23 Crespo-Quesada M, Dykeman RR, Laurenczy G, Dyson PJ and Kiwi-Minsker L, Supported nitrogen-modified Pd nanoparticles for the selective hydrogenation of 1-hexyne. *J Catal* **279**:66–74 (2011).
24 Maccarrone MJ, Lederhos C, Badano J, Quiroga ME and Yori JC, *Avances Ciencias Ingeniería* **2**:59–68 (2011).
25 L'Argentière PC and Fígoli NS, Pd-W and Pd-Co bimetallic catalysts' sulfur resistance for selective. hydrogenation. *Ind Eng Chem Res* **36**:2543–2546 (1997).
26 NIST X-ray Photoelectron Spectroscopy Database NIST Standard Reference Database 20, Version 3.5 (2007) (Web version) National Institute of Standards and Technology, USA, http://srdata.nist.gov/xps/[accessed in Feb 2011].
27 Wang CB, Lin HK and Ho CM, Effects of the addition of titania on the thermal characterization of alumina-supported palladium. *J Mol Catal A: Chem* **180**:285–291 (2002).
28 Benitez VM, Querini CA, Fígoli NS and Comelli RA, Skeletal isomerization of 1-butene on WO_x/gamma-Al_2O_3. *Appl Catal A: Gen* **178**:205–218 (1999).
29 Martin C, Solana G, Malet P and Rives V, Nb_2O_5-supported WO_3. A comparative study with WO_3/Al_2O_3. *Catal Today* **78**:365–376 (2003).
30 Huang S, Zhang C and He H, Complete oxidation of o-xylene over Pd/Al_2O_3 catalyst at low temperature. *Catal Today* **139**:15–23 (2008).
31 Benitez VM and Fígoli NS, About the importance of surface W species in WO_x/Al_2O_3 during n-butene skeletal isomerization. *Catal Comm* **3**:487–492 (2002).
32 Contreras JL, Fuentes GA, Zeifert B and Salmones J, Stabilization of supported platinum nanoparticles on gamma alumina catalysts by addition of tungsten. *J Alloys Compd* **483**:371–376 (2009).
33 Cruz J, Avalos-Borja M, López Cordero R, Bañares MA and Fierro JLG, Influence of pH of the impregnation solution on the phosphorus promotion in W/Al_2O_3 hydrotreating catalysts. *Appl Catal A: Gen* **224**:97–110 (2002).
34 Logie V, Maire G, Michel D and Vignes JL, Skeletal isomerization of hexenes on tungsten oxide supported on porous α-alumina. *J Catal* **188**:90–101 (1999).
35 Joback KG, Unified approach to physical property estimation using multivariate statistical techniques. MS thesis, MIT, Cambridge, MA (1984).
36 Semagina N, Renken A and Kiwi-Minsker L, Monodispersed Pd-nanoparticles on carbon fiber fabrics as structured catalyst for selective hydrogenation. *Chem Eng Sci* **62**:5344–5348 (2007).

